Editors' Suggestion | Featured in Physics

Frequency Stability of 2.5×10^{-17} from a Si Cavity with AlGaAs Crystalline Mirrors

Dahyeon Lee,[1,*] Zoey Z. Hu,[1] Ben Lewis,[1] Alexander Aeppli,[1] Kyungtae Kim,[1] Zhibin Yao,[1] Thomas Legero,[2] Daniele Nicolodi,[2] Fritz Riehle,[2] Uwe Sterr,[2] and Jun Ye[1,†]

[1]*JILA, National Institute of Standards and Technology and the University of Colorado, Boulder, Colorado 80309-0440, USA and Department of Physics, University of Colorado, Boulder, Colorado 80309-0390, USA*

[2]*Physikalisch-Technische Bundesanstalt, Bundesallee 100, 38116 Braunschweig, Germany*

(Received 16 September 2025; accepted 8 December 2025; published 20 January 2026)

Developments in ultrastable lasers have fueled remarkable advances in optical frequency metrology and quantum science. A key ingredient in further improving laser frequency stability is the use of low-noise mirror materials such as AlGaAs crystalline coatings. However, excess noise observed with these coatings limits the performance of cryogenic silicon cavities with AlGaAs mirrors to similar levels achieved with conventional dielectric coatings. With a new pair of crystalline coated mirrors in a 6-cm-long cryogenic silicon cavity operated at 17 K, we demonstrate a clear advantage of crystalline coatings over dielectric coatings. The achieved fractional frequency stability of 2.5×10^{-17} at 10 s is four times better than expected for dielectric mirrors and corresponds to more than a tenfold reduction in the coating mechanical loss factor. We also combine two silicon cavities to demonstrate optical frequency averaging for enhanced stability. In addition, we present a long-term frequency drift record of four cryogenic silicon cavities measured over several years. These results open up realistic prospects for cavity-stabilized lasers with 10^{-18} fractional stability, as well as an all-optical timescale with continuously operating optical local oscillators.

DOI: 10.1103/zgrm-cjbb

Introduction—Ultrastable optical interferometers form the backbone of optical atomic clocks [1], tabletop tests of fundamental physics [2–5], and gravitational wave detectors [6,7]. Cryogenic silicon cavities continue to push the state of the art in optical frequency stability, reaching thermal noise-limited fractional frequency stability of 3.5×10^{-17} up to thousands of seconds [8,9]. Despite this impressive performance, cavity-stabilized laser frequency noise is still the limiting factor in improving optical clock stability. To improve the frequency stability of optical cavities even further, the fundamental Brownian thermal noise of the mirror coatings needs to be mitigated, for example, by going to lower temperatures [4,10–13], enlarging the mode area, utilizing novel mirror coating materials that exhibit lower Brownian noise [14–17], or indirectly scaling down the noise contribution by using a longer cavity [18–20]. While all of these approaches are actively pursued, mirror coatings based on stacks of crystalline GaAs/AlGaAs have recently attracted significant attention [11,14,21–26], with possible applications reaching as far as next-generation gravitational wave detectors [27]. These mirrors have lower thermal noise compared to conventional dielectric mirrors due to their lower mechanical loss factor [28–30], and can achieve the high finesse critically required for ultrastable optical cavities. These desirable qualities make crystalline mirrors an attractive candidate to replace conventional dielectric mirror coatings for high-performance optical cavities.

However, our previous investigations on cryogenic silicon cavities with crystalline mirrors revealed several novel noise mechanisms that hinder reaching the Brownian thermal noise [21,22]. One of the excess noise sources was found to be associated with the birefringence of the crystalline coatings, in which two birefringently split cavity modes showed anticorrelated noise at a level significantly higher than the expected thermal noise. Although the birefringent noise could be suppressed to a sufficiently low level by averaging the frequencies of the two cavity modes, the thermal noise floor of the crystalline coatings still could not be reached because of yet another source of excess "global" noise that appeared in two independent systems at JILA and PTB. Unlike the Brownian noise, whose correlation length is on the order of the μm-scale coating thickness, the global noise was correlated over the mm-scale mode area and thus could not be lowered by using a larger mode size [22]. The origin of the excess noise is not clear and may be related to coating impurities, defects, or variations in the bond strength, while it could also be the thermal noise of the mirror optical contact area and the cavity supports. Because of this excess global noise, the frequency stabilities of cryogenic silicon cavities with crystalline mirrors have been limited to levels comparable to those of similar cavities with conventional dielectric mirrors, leaving the full potential of crystalline mirrors unfulfilled.

*Contact author: dahyeon.lee@colorado.edu
†Contact author: ye@jila.colorado.edu

In this Letter, with a 17 K cryogenic silicon cavity, we demonstrate for the first time clear superiority of crystalline $Al_{0.92}Ga_{0.08}As$ coatings over conventional dielectric mirrors. The frequency stability of 2.5×10^{-17}, expressed in modified Allan deviation, is a factor of 4 better than the thermal noise limit of an equivalent cavity with conventional dielectric SiO_2/Ta_2O_5 coatings. In addition, we implement optical frequency averaging of two state-of-the-art silicon cavities to improve frequency stability. Finally, we compare the long-term drift rates of four silicon cavities in PTB and JILA compiled over more than ten years.

Frequency stability—Our 6-cm-long silicon cavity uses two 1 m radius of curvature mirrors made of alternating layers of crystalline GaAs/AlGaAs on a silicon substrate. The 12.0-μm-thick crystalline mirror coating comprises 48.5 repeats of quarter-wave high-index GaAs and low-index $Al_{0.92}Ga_{0.08}As$ layers, beginning and ending with the GaAs layer. The cavity finesse is 470 000 at the operating wavelength of 1542 nm, corresponding to a cavity linewidth of 5 kHz. The double-cone shaped cavity is vertically mounted from its midplane to reduce vibration sensitivity [31]. Vibration noise from the cryostat is mitigated with the split-plate design and an active vibration isolation table as described in Refs. [10,32], so that vibration noise does not degrade cavity performance at Fourier frequencies below 3 Hz except for discrete peaks at harmonics of the 1 Hz cryostat cycle frequency. The cavity is cooled with a closed-cycle cryostat to 17 K, where the coefficient of thermal expansion of silicon is zero [33]. Thermal isolation from the environment is achieved with multiple layers of shielding, including a radiation shield, an actively controlled outer shield, and a passive inner shield. A 1542 nm fiber laser is locked to the cavity with the Pound-Drever-Hall technique [34,35]. Residual amplitude modulation (RAM) is actively suppressed well below the cavity thermal noise limit with the AOM FM-triplet scheme described in Ref. [36], which allows us to operate the system at shot noise-limited signal-to-noise ratio with just 90 nW of cavity transmission. The birefringent noise of the crystalline mirrors is canceled by simultaneously locking to two orthogonal polarization modes of the cavity [21,22]. Without the dual-polarization lock, the laser fractional frequency stability is severely degraded to low-10^{-16} level. A technical noise budget for the system is reported elsewhere [21], with the only difference being the RAM cancellation scheme [36].

The fractional frequency stability of the 6-cm cavity is shown in Fig. 1. Linear drift is removed from all datasets. The frequency stability for averaging times less than 100 s (filled markers) is measured with the three-cornered-hat method [37], using a 21-cm silicon cavity and a 40-cm ultralow-expansion (ULE) glass cavity as the other two references [9,38,39]. The trace shown is the average of 10 separate three-cornered-hat measurements each lasting 5 h, and the shaded area marks the full range of observed values. For averaging times longer than 100 s,

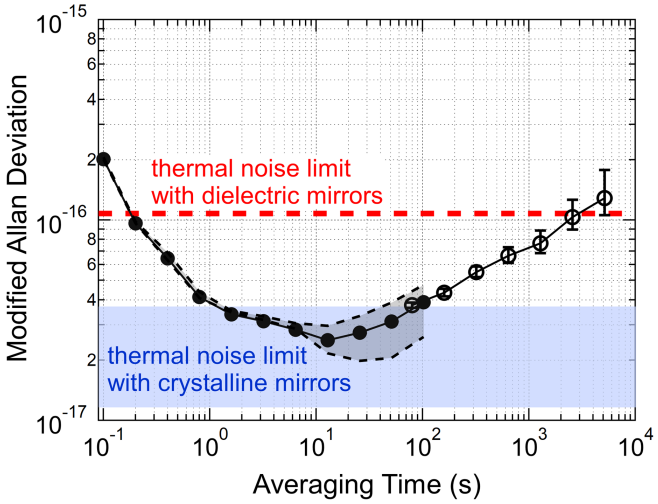

FIG. 1. Fractional frequency stability of the 6-cm silicon cavity with crystalline mirrors at 17 K. The use of crystalline mirrors results in a significant reduction of the cavity thermal noise (from red dashed line to blue shaded area, see text). For averaging times less than 100 s, the average of ten three-cornered-hat measurements each lasting 5 h is shown (filled markers). The gray shaded area shows the full range of these ten independent measurements. For averaging times longer than 100 s, the cavity frequency is measured with a Sr lattice clock (empty markers). Linear drift is removed in all datasets.

the three-cornered-hat method yields unreliable results due to the relatively high instability of the ULE cavity, so a Sr lattice clock is used for long term measurements (empty markers) [40]. The measured frequency stability of 2.5×10^{-17} around 10 s of averaging is four times lower than the expected Brownian thermal noise of conventional dielectric coatings, clearly demonstrating the superior noise performance of crystalline mirrors. The short term performance of the 6-cm cavity (< 1 s averaging time, see End Matter) is worse than that of the 21-cm cavity [9,41], due to excess technical noise sources such as cryostat vibrations.

The expected thermal noise level of crystalline mirrors has a large uncertainty because the mechanical loss factor of the coatings is not well characterized, especially at the 17 K operating temperature of our cavity. Published loss factors from mechanical ringdown measurements range from 6×10^{-6} to 5×10^{-5} in this temperature range [42–44], with the correspondingly large uncertainty range of thermal noise displayed as the blue shaded area in Fig. 1. The observed modified Allan deviation of 2.5×10^{-17} around 10 s places an upper bound on the 17 K loss of crystalline coatings at 2.3×10^{-5}, which is more than a factor of 10 lower than the 17 K loss of conventional dielectric coatings of 3.2×10^{-4} [45].

Our previous work on crystalline mirrors confirmed the well-known room temperature loss factor of 2.5×10^{-5} at 124 K by measuring the differential Brownian thermal noise between the HG_{00} and HG_{01} spatial modes of the

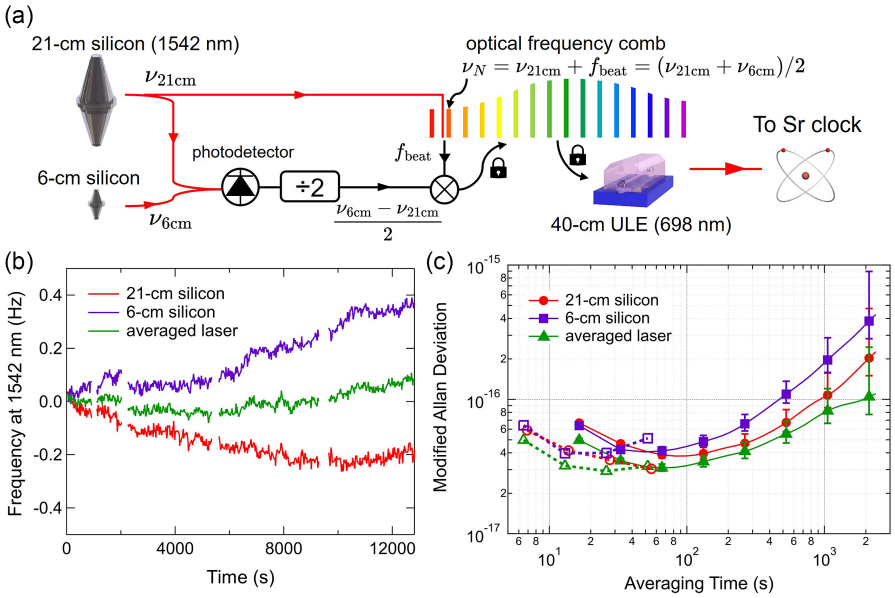

FIG. 2. Optical frequency averaging of light using two silicon cavities. (a) Schematic diagram of the setup. By phase locking f_{beat}, the beat note between the comb and the 21-cm silicon cavity, to a separately generated $(\nu_{6\ \mathrm{cm}} - \nu_{21\ \mathrm{cm}})/2$, the comb is stabilized to the average frequency of the two silicon cavities. A 698 nm laser locked to the 40-cm ULE cavity is further stabilized to the comb and interrogates Sr atoms. (b) Frequency record of the lasers locked to the 21-cm cavity, 6-cm cavity, and the averaged laser, measured with the Sr clock. (c) Modified Allan deviation of the three lasers computed from the data in (b) (solid lines). The relatively high instability at short averaging times is from Dick noise, which is verified by operating the clock with a shorter dead time, hence less Dick noise (dotted lines).

same cavity [22,28]. We however identified excess global noise, which was measured in two independent silicon cavities operated at 124 and 17 K [21,22], that was nearly identical when expressed in terms of displacement noise after scaling the fractional frequency noise by the respective cavity lengths. This leads us to attribute this noise source to the mirror coatings.

We do not observe the excess global noise in the current 6-cm cavity system, which is nominally identical to the one used in our previous publications but with different mirrors. The crystalline mirrors used in Refs. [21,22], manufactured in 2017, were replaced with a new pair of crystalline mirrors in 2023. No modification was made to the composition of the coating material and the growth process, so the change in global noise is not understood and further investigation is needed to uncover the origin of the global noise of the 2017 coating. The new crystalline mirrors have a lower transmission than the previous mirrors by using a GaAs/AlGaAs stack with three more periods, increasing the coating thickness from 11.3 μm to 12.0 μm. As optical loss from scattering and absorption remains the same at approximately 5 ppm per mirror, finesse increases from 290 000 to 470 000. The birefringent mode splitting also changed from 770 to 890 kHz with the new set of mirrors.

Optical frequency averaging—With two state-of-the-art cryogenic silicon cavities online at JILA, we improved the laser stability even further by averaging the two cavities. While the idea of combining two or more oscillators to achieve better performance is not new [41,46–48], it is especially valuable when applied to state-of-the-art silicon cavities because building a new cavity with improved performance is not trivial when the cavity is already at the record performance level.

Figure 2(a) shows how optical frequency averaging is implemented. A 1542-nm laser stabilized to the 21-cm cavity is heterodyned with a self-referenced Er:fiber frequency comb such that the nearest comb mode frequency can be written as $\nu_N = \nu_{21\ \mathrm{cm}} + f_{\mathrm{beat}}$, where ν_N is the optical frequency of the N^{th} comb mode, $\nu_{21\ \mathrm{cm}}$ is the optical frequency of the laser locked to the 21-cm silicon cavity, and f_{beat} is the rf beat note between the two optical frequencies. For normal operation, f_{beat} is phase locked to a synthesizer by feeding back to the comb, thereby transferring the stability of the 21-cm silicon cavity to the comb. A 698-nm laser prestabilized to the 40-cm ULE cavity is then phase locked to the comb and interrogates Sr atoms. For optical frequency averaging, a simple modification is made to the phase locking scheme. Instead of locking f_{beat} to a synthesizer, it is locked to $(\nu_{6\ \mathrm{cm}} - \nu_{21\ \mathrm{cm}})/2$ generated with an rf frequency divider, where $\nu_{6\ \mathrm{cm}}$ is the optical frequency of the 6-cm silicon cavity. With this modification, the comb mode frequency becomes $\nu_N = (\nu_{21\ \mathrm{cm}} + \nu_{6\ \mathrm{cm}})/2$, i.e., the average frequency of the two cavities. The comb can also be locked to the 6-cm cavity by bypassing the divide-by-two operation.

The frequencies of the lasers locked to the two silicon cavities and their average frequency, measured with the

Sr lattice clock are shown in Fig. 2(b). The laser frequencies are measured with three independent, interleaved feedback loops that steer the laser frequencies to the Sr clock transition. The interleaving is achieved by switching the laser that interrogates the Sr atoms for consecutive cycles of the Sr clock. The action of the averaging operation is clearly seen in the cancellation of the opposite-sign drifts of the two cavities. The solid lines in Fig. 2(c) show the modified Allan deviation corresponding to the data in Fig. 2(b). The averaged laser is more stable than the two similar individual lasers by approximately $\sqrt{2}$, consistent with expectation. The measurement at short averaging times is limited by Dick noise due to the long dead time inherent to interleaved measurements [49]. To verify this, we reduce the dead time by measuring the three lasers independently against Sr atoms without interleaving, shown in dashed lines. As expected, the Dick noise contribution is reduced at shorter averaging times.

A more stable local oscillator corresponds to improved clock stability for a Dick noise-limited clock such as ours, evidenced by the reduced Dick noise of the averaged laser in Fig. 2(c). Because of the improved clock stability, evaluation of systematic clock uncertainties can be performed twice as fast with a $\sqrt{2}$ times lower instability of the local oscillator. Furthermore, the longer laser coherence time allows a longer clock interrogation time, reducing the instability due to quantum projection noise [50,51].

Drift of silicon cavities—The drift rate of cryogenic silicon cavities is orders of magnitude lower than that of ULE cavities. While typical ULE cavities drift a few kilohertz per day, cryogenic silicon cavities drift only a few hertz per day. It is currently unknown where this small amount of drift comes from. Unlike ULE cavities whose spacers are made of amorphous glass material that can relax over time, silicon cavities are made of crystalline material and therefore should not drift at all in principle. Silicon cavities with crystalline coatings are especially interesting because even the mirror coatings are crystalline, making the entire cavity crystalline. To shed light on the origin of the drift, we report the long-term drift rates of four silicon cavities currently operating at PTB and JILA, accumulated over more than ten years. The naming convention of the four cavities and their relevant features, as well as previous publications, are summarized in Table I.

TABLE I. Four cryogenic silicon cavities at JILA and PTB whose drift rates are reported in this Letter.

Name	Length	Temperature	Mirror material	References
Si2	21 cm	124 K	SiO_2/Ta_2O_5	[9]
Si3	21 cm	124 K	SiO_2/Ta_2O_5	[8,9]
Si5	21 cm	124 K	$GaAs/Al_{0.92}Ga_{0.08}As$	[21,22]
Si6[a]	6 cm	17 K	$GaAs/Al_{0.92}Ga_{0.08}As$	[21,22]

[a]As noted in the main text, the results reported in this Letter are obtained with a new set of crystalline mirrors than the ones used in Refs. [21,22].

Figure 3(a) shows the coefficient of thermal expansion of silicon over a range of temperatures [33,52]. To suppress cavity length changes from temperature fluctuations, the silicon cavities operate at zero crossings of the coefficient of thermal expansion. Three of the four cavities reported here (Si2, Si3, Si5) operate at the 124 K zero crossing. Si6, on the other hand, operates at the 17 K zero crossing [Fig. 3(a) inset], where the much gentler slope of the coefficient of thermal expansion significantly relaxes the requirements on temperature stability.

The long term drift rates of the silicon cavities are shown in Fig. 3(b). The origin of the horizontal axis is chosen to be the day each cavity was assembled by optical contact bonding the mirrors to the spacer, as a representative for the "age" of the cavity. The absolute frequencies of the cavities are tracked with hydrogen masers or optical clocks. For Si2, Si3, and Si5, the drift rates are calculated by first computing a ten-day binned average of the cavity frequency and then taking the derivative. For Si6, the system

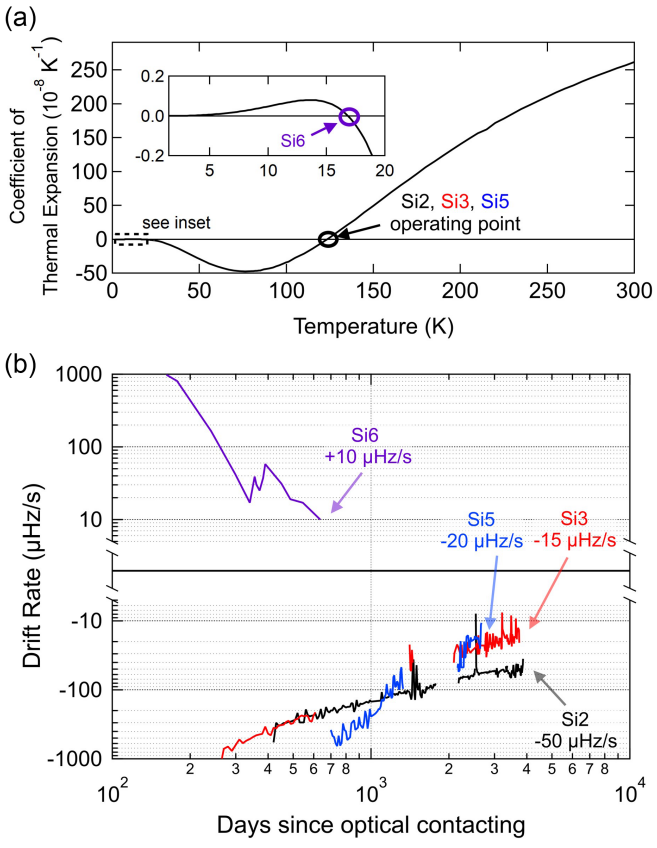

FIG. 3. Coefficient of thermal expansion of silicon and long-term drift rates of the four cryogenic silicon cavities in Table I. (a) Coefficient of thermal expansion of silicon. The data between 1.5 and 24 K are from Ref. [33] and between 24 and 300 K are from Ref. [52]. (b) Drift rates of the four silicon cavities (Black: Si2; Red: Si3; Blue: Si5; Purple: Si6). All four cavities exhibit very low drift rates in the tens of microhertz per second range.

was still being optimized for a large portion of the dates plotted here such that 10-day averaging was not appropriate. The Si6 drift rate is therefore calculated over durations ranging from 1 to 24 days. After several years, all of the silicon cavities settle to drift rates in the tens of microhertz per second range. Some distinguishing features can be observed in the drift rate of the 6-cm cavity Si6, although the record to date spans less than two years. First, the sign of the drift rate is opposite from that of all the other silicon cavities. The effective cavity length of Si6 is getting shorter over time, similar to the drift behavior of glass and ceramic cavities [19,53–57]. Second, the drift rate of Si6 settles to a low value much faster than the other cavities. All three other cavities took several years until the drift rate reached tens of microhertz per second level whereas Si6 took less than two years before reaching a similar drift rate.

To put these drift rates into context, we note that the absolute frequency of Si2, the cavity whose frequency has been tracked the longest, has drifted only −44 kHz in the past ten years. Converted to cavity length change, this corresponds to an overall lengthening of the 21-cm cavity by 48 pm, which is approximately 1/11 of the silicon lattice constant. The recent drift rates of −50 μHz/s (-2.6×10^{-19} s^{-1} in fractional units), −15 μHz/s (-7.7×10^{-20} s^{-1}), −20 μHz/s (-1.0×10^{-19} s^{-1}), and 10 μHz/s (5.2×10^{-20} s^{-1}) of Si2, Si3, Si5, and Si6, respectively, are nearly competitive with typical fractional drift rates of active hydrogen masers in the 10^{-21}–10^{-20} s^{-1} range [58–60]. Further stability improvements in the range of 10^4 to 10^6 s will open up the possibility of an all-optical timescale using optical cavities and optical clocks [61–64].

As mentioned previously, the mechanism that causes the drift in cryogenic silicon cavities, let alone its sign and settling behavior, is currently unknown. Possible mechanisms include slow relaxation of the stress induced by cavity mounting structure, optically contacted surfaces [54,65], or mirror coatings [66]. Further investigations and new cryogenic silicon cavities at different operating temperatures might provide more insight into the origin of this drift behavior [4,13].

Conclusion—The fractional frequency stability of cavity-stabilized lasers now reaches an impressive 10^{-17} level, yet still limits the stability of optical clocks. An important step towards next-generation optical cavities is the development of low mechanical loss semiconductor crystalline mirrors. In this Letter, we demonstrate a record fractional frequency stability of 2.5×10^{-17} for any optical reference cavity. This corresponds to mirror displacement stability of 1.5×10^{-18} m for a 6-cm cavity length, and we extract an upper bound on the mechanical loss factor of 2.3×10^{-5} at 17 K, confirming expectations on the superior mechanical properties of crystalline AlGaAs coatings over dielectric coatings. We also demonstrate optical frequency averaging of two silicon cavities, resulting in an optical frequency that is more stable than its constituents both at short and long averaging times. In addition, the long-term drift rates of four silicon cavities over several years are reported. By combining the key properties already realized in this and other silicon cavities, namely, 21 cm length, 17 K operation, large radius of curvature mirrors, and crystalline coatings, we anticipate a cryogenic silicon cavity with low-10^{-18} performance to be practically feasible.

Acknowledgments—We thank Y. Yang, E. Y. Song, and S. Agrawal for providing insightful comments on the manuscript. We acknowledge contributions and discussions from G. D. Cole, G.-W. Truong, and W. Warfield. Funding for this work is provided by NSF No. QLCI OMA-2016244, V. Bush Fellowship, NSF No. PHY-2317149, and NIST. Authors at PTB acknowledge support by the Deutsche Forschungsgemeinschaft (DFG, German Research Foundation) under Germany's Excellence Strategy–EX-2123 QuantumFrontiers (Project No. 390837967) and by the Max Planck-RIKEN-PTB Center for Time, Constants and Fundamental Symmetries.

Data availability—The data that support the findings of this article are openly available [67].

[1] A. D. Ludlow, M. M. Boyd, J. Ye, E. Peik, and P. O. Schmidt, Optical atomic clocks, Rev. Mod. Phys. **87**, 637 (2015).
[2] C. J. Kennedy, E. Oelker, J. M. Robinson, T. Bothwell, D. Kedar, W. R. Milner, G. E. Marti, A. Derevianko, and J. Ye, Precision metrology meets cosmology: Improved constraints on ultralight dark matter from atom-cavity frequency comparisons, Phys. Rev. Lett. **125**, 201302 (2020).
[3] H. Müller, S. Herrmann, C. Braxmaier, S. Schiller, and A. Peters, Modern Michelson-Morley experiment using cryogenic optical resonators, Phys. Rev. Lett. **91**, 020401 (2003).
[4] E. Wiens, A. Y. Nevsky, and S. Schiller, Resonator with ultrahigh length stability as a probe for equivalence-principle-violating physics, Phys. Rev. Lett. **117**, 271102 (2016).
[5] P. Wcisło, P. Morzyński, M. Bober, A. Cygan, D. Lisak, R. Ciuryło, and M. Zawada, Experimental constraint on dark matter detection with optical atomic clocks, Nat. Astron. **1**, 0009 (2016).
[6] G. M. Harry, H. Armandula, E. Black, D. Crooks, G. Cagnoli, J. Hough, P. Murray, S. Reid, S. Rowan, P. Sneddon *et al.*, Thermal noise from optical coatings in gravitational wave detectors, Appl. Opt. **45**, 1569 (2006).
[7] R. X. Adhikari, K. Arai, A. Brooks, C. Wipf, O. Aguiar, P. Altin, B. Barr, L. Barsotti, R. Bassiri, A. Bell *et al.*, A cryogenic silicon interferometer for gravitational-wave detection, Classical Quantum Gravity **37**, 165003 (2020).
[8] E. Oelker, R. Hutson, C. Kennedy, L. Sonderhouse, T. Bothwell, A. Goban, D. Kedar, C. Sanner, J. Robinson, G. Marti *et al.*, Demonstration of 4.8×10^{-17} stability at 1 s for two independent optical clocks, Nat. Photonics **13**, 714 (2019).
[9] D. G. Matei, T. Legero, S. Häfner, C. Grebing, R. Weyrich, W. Zhang, L. Sonderhouse, J. M. Robinson, J. Ye, F. Riehle,

and U. Sterr, 1.5 μm lasers with sub-10 mHz linewidth, Phys. Rev. Lett. **118**, 263202 (2017).
[10] J. M. Robinson, E. Oelker, W. R. Milner, W. Zhang, T. Legero, D. G. Matei, F. Riehle, U. Sterr, and J. Ye, Crystalline optical cavity at 4 K with thermal-noise-limited instability and ultralow drift, Optica **6**, 240 (2019).
[11] J. Valencia, G. Iskander, N. V. Nardelli, D. R. Leibrandt, and D. B. Hume, Cryogenic sapphire optical reference cavity with crystalline coatings at 1×10^{-16} fractional frequency instability, Rev. Sci. Instrum. **95**,103002 (2024).
[12] L. He, J. Zhang, Z. Wang, J. Chang, Q. Wu, Z. Lu, and J. Zhang, Ultra-stable cryogenic sapphire cavity laser with an instability reaching 2×10^{-16} based on a low vibration level cryostat, Opt. Lett. **48**, 2519 (2023).
[13] J. Barbarat, J. Gillot, J. Millo, C. Lacroûte, T. Legero, V. Giordano, and Y. Kersalé, Towards a sub-kelvin cryogenic Fabry-Perot silicon cavity, J. Phys. Conf. Ser. **2889**, 012056 (2024).
[14] G. D. Cole, W. Zhang, M. J. Martin, J. Ye, and M. Aspelmeyer, Tenfold reduction of Brownian noise in high-reflectivity optical coatings, Nat. Photonics **7**, 644 (2013).
[15] G.-W. Truong, L. W. Perner, D. M. Bailey, G. Winkler, S. B. Cataño-Lopez, V. J. Wittwer, T. Südmeyer, C. Nguyen, D. Follman, A. J. Fleisher *et al.*, Mid-infrared supermirrors with finesse exceeding 400 000, Nat. Commun. **14**, 7846 (2023).
[16] J. Dickmann, S. Sauer, J. Meyer, M. Gaedtke, T. Siefke, U. Brückner, J. Plentz, and S. Kroker, Experimental realization of a 12,000-finesse laser cavity based on a low-noise microstructured mirror, Commun. Phys. **6**, 16 (2023).
[17] G. M. Harry, M. R. Abernathy, A. E. Becerra-Toledo, H. Armandula, E. Black, K. Dooley, M. Eichenfield, C. Nwabugwu, A. Villar, D. Crooks *et al.*, Titania-doped tantala/silica coatings for gravitational-wave detection, Classical Quantum Gravity **24**, 405 (2006).
[18] S. Häfner, S. Falke, C. Grebing, S. Vogt, T. Legero, M. Merimaa, C. Lisdat, and U. Sterr, 8×10^{-17} fractional laser frequency instability with a long room-temperature cavity, Opt. Lett. **40**, 2112 (2015).
[19] M. D. Álvarez, *Optical Cavities for Optical Atomic Clocks, Atom Interferometry and Gravitational-Wave Detection* (Springer, New York, 2019).
[20] A. L. Parke and M. Schioppo, Three hundred microsecond optical cavity storage time and 10^{-7} active RAM cancellation for 10^{-19} laser frequency stabilization, Opt. Lett. **50**, 3405 (2025).
[21] D. Kedar, J. Yu, E. Oelker, A. Staron, W. R. Milner, J. M. Robinson, T. Legero, F. Riehle, U. Sterr, and J. Ye, Frequency stability of cryogenic silicon cavities with semiconductor crystalline coatings, Optica **10**, 464 (2023).
[22] J. Yu, S. Häfner, T. Legero, S. Herbers, D. Nicolodi, C. Y. Ma, F. Riehle, U. Sterr, D. Kedar, J. M. Robinson *et al.*, Excess noise and photoinduced effects in highly reflective crystalline mirror coatings, Phys. Rev. X **13**, 041002 (2023).
[23] S. Herbers, S. Häfner, S. Dörscher, T. Lücke, U. Sterr, and C. Lisdat, Transportable clock laser system with an instability of 1.6×10^{-16}, Opt. Lett. **47**, 5441 (2022).
[24] B. Kraus, S. Herbers, C. Nauk, U. Sterr, C. Lisdat, and P. O. Schmidt, Ultra-stable transportable ultraviolet clock laser using cancellation between photo-thermal and photo-birefringence noise, Opt. Lett. **50**, 658 (2025).
[25] X.-Q. Zhu, X.-Y. Cui, D.-Q. Kong, H.-W. Yu, X.-M. Zhai, M.-Y. Zheng, X.-P. Xie, Q. Zhang, X. Jiang, X.-B. Zhang *et al.*, An ultrastable 1397-nm laser stabilized by a crystalline-coated room-temperature cavity, Rev. Sci. Instrum. **95**, 083002 (2024).
[26] A. Didier, J. Millo, B. Marechal, C. Rocher, E. Rubiola, R. Lecomte, M. Ouisse, J. Delporte, C. Lacroûte, and Y. Kersalé, Ultracompact reference ultralow expansion glass cavity, Appl. Opt. **57**, 6470 (2018).
[27] G. D. Cole, S. Ballmer, G. Billingsley, S. Cataño-Lopez, M. Fejer, P. Fritschel, A. Gretarsson, G. Harry, D. Kedar, T. Legero *et al.*, Substrate-transferred GaAs/AlGaAs crystalline coatings for gravitational-wave detectors, Appl. Phys. Lett. **122**, 110502 (2023).
[28] S. D. Penn, M. M. Kinley-Hanlon, I. A. MacMillan, P. Heu, D. Follman, C. Deutsch, G. D. Cole, and G. M. Harry, Mechanical ringdown studies of large-area substrate-transferred GaAs/AlGaAs crystalline coatings, J. Opt. Soc. Am. B **36**, C15 (2019).
[29] K. Numata, A. Kemery, and J. Camp, Thermal-noise limit in the frequency stabilization of lasers with rigid cavities, Phys. Rev. Lett. **93**, 250602 (2004).
[30] T. Kessler, T. Legero, and U. Sterr, Thermal noise in optical cavities revisited, J. Opt. Soc. Am. B **29**, 178 (2011).
[31] M. Notcutt, L.-S. Ma, J. Ye, and J. L. Hall, Simple and compact 1-Hz laser system via an improved mounting configuration of a reference cavity, Opt. Lett. **30**, 1815 (2005).
[32] W. Zhang, J. M. Robinson, L. Sonderhouse, E. Oelker, C. Benko, J. L. Hall, T. Legero, D. G. Matei, F. Riehle, U. Sterr, and J. Ye, Ultrastable silicon cavity in a continuously operating closed-cycle cryostat at 4 K, Phys. Rev. Lett. **119**, 243601 (2017).
[33] E. Wiens, Q.-F. Chen, I. Ernsting, H. Luckmann, U. Rosowski, A. Nevsky, and S. Schiller, Silicon single-crystal cryogenic optical resonator, Opt. Lett. **39**, 3242 (2014).
[34] R. W. Drever, J. L. Hall, F. V. Kowalski, J. Hough, G. Ford, A. Munley, and H. Ward, Laser phase and frequency stabilization using an optical resonator, Appl. Phys. B **31**, 97 (1983).
[35] E. D. Black, An introduction to Pound–Drever–Hall laser frequency stabilization, Am. J. Phys. **69**, 79 (2001).
[36] D. Kedar, Z. Yao, I. Ryger, J. L. Hall, and J. Ye, Synthetic FM triplet for AM-free precision laser stabilization and spectroscopy, Optica **11**, 58 (2024).
[37] J. Gray and D. Allan, in *Proceedings of the 28th Annual Symposium on Frequency Control, Atlantic City, New Jersey, New Jersey* (Electronic Industries Association, Atlantic City, NJ, 1974), pp. 243–246.
[38] M. D. Swallows, M. J. Martin, M. Bishof, C. Benko, Y. Lin, S. Blatt, A. M. Rey, and J. Ye, Operating a ^{87}Sr optical lattice clock with high precision and at high density, IEEE Trans. Ultrasonics Ferroelectr. Freq. Control **59**, 416 (2012).
[39] T. L. Nicholson, M. J. Martin, J. R. Williams, B. J. Bloom, M. Bishof, M. D. Swallows, S. L. Campbell, and J. Ye, Comparison of two independent Sr optical clocks with 1×10^{-17} stability at 10^3 s, Phys. Rev. Lett. **109**, 230801 (2012).
[40] A. Aeppli, K. Kim, W. Warfield, M. S. Safronova, and J. Ye, Clock with 8×10^{-19} systematic uncertainty, Phys. Rev. Lett. **133**, 023401 (2024).
[41] L. Yan, S. Lannig, W. R. Milner, M. N. Frankel, B. Lewis, D. Lee, K. Kim, and J. Ye, High-power clock laser spectrally

tailored for high-fidelity quantum state engineering, Phys. Rev. X **15**, 031055 (2025).
[42] G. D. Cole, S. Gröblacher, K. Gugler, S. Gigan, and M. Aspelmeyer, Monocrystalline $Al_xGa_{1-x}As$ heterostructures for high-reflectivity high-Q micromechanical resonators in the megahertz regime, Appl. Phys. Lett. **92**, 261108 (2008).
[43] G. D. Cole, Cavity optomechanics with low-noise crystalline mirrors, in *Optical Trapping and Optical Micromanipulation IX* (SPIE, San Diego, CA, 2012), Vol. 8458, pp. 28–38.
[44] R. Pagano, S. Aronson, T. Cullen, G. D. Cole, and T. Corbitt, Thermal noise measurement below the standard quantum limit, arXiv:2507.02196.
[45] J. M. Robinson, E. Oelker, W. R. Milner, D. Kedar, W. Zhang, T. Legero, D. G. Matei, S. Häfner, F. Riehle, U. Sterr *et al.*, Thermal noise and mechanical loss of SiO_2/Ta_2O_5 optical coatings at cryogenic temperatures, Opt. Lett. **46**, 592 (2021).
[46] L. Yan, Y. Zhang, Z. Tai, P. Zhang, X. Zhang, W. Guo, S. Zhang, and H. Jiang, Multi-cavity-stabilized ultrastable laser, Chin. Optic. Lett. **16**, 121403 (2018).
[47] W. Loh, R. T. Maxson, A. P. Medeiros, G. N. West, P. W. Juodawlkis, and R. P. McConnell, Optical frequency averaging of light, Opt. Express **31**, 25507 (2023).
[48] R. Schwarz, S. Dörscher, A. Al-Masoudi, E. Benkler, T. Legero, U. Sterr, S. Weyers, J. Rahm, B. Lipphardt, and C. Lisdat, Long term measurement of the ^{87}Sr clock frequency at the limit of primary Cs clocks, Phys. Rev. Res. **2**, 033242 (2020).
[49] G. J. Dick, Local oscillator induced instabilities in trapped ion frequency standards, in *Proceedings of the 19th Annual Precise Time and Time Interval Systems and Applications Meeting* (Redondo Beach, CA, 1989), pp. 133–147.
[50] M. C. Marshall, Daniel A. Rodriguez Castillo, W. J. Arthur-Dworschack, A. Aeppli, K. Kim, D. Lee, W. Warfield, J. Hinrichs, N. V. Nardelli, T. M. Fortier, J. Ye, D. R. Leibrandt, and D. B. Hume, High-stability single-ion clock with 5.5×10^{-19} systematic uncertainty, Phys. Rev. Lett. **135**, 033201 (2025).
[51] M. E. Kim, W. F. McGrew, N. V. Nardelli, E. R. Clements, Y. S. Hassan, X. Zhang, J. L. Valencia, H. Leopardi, D. B. Hume, T. M. Fortier *et al.*, Improved interspecies optical clock comparisons through differential spectroscopy, Nat. Phys. **19**, 25 (2023).
[52] K. G. Lyon, G. L. Salinger, C. A. Swenson, and G. White, Linear thermal expansion measurements on silicon from 6 to 340 K, J. Appl. Phys. **48**, 865 (1977).
[53] T. Legero, T. Kessler, and U. Sterr, Tuning the thermal expansion properties of optical reference cavities with fused silica mirrors, J. Opt. Soc. Am. B **27**, 914 (2010).
[54] J. L. Hall, Frequency-stabilized lasers: A parochial review, in *Frequency-Stabilized Lasers and Their Applications* (SPIE, Boston, MA, 1993), Vol. 1837, pp. 2–15.
[55] P. Dubé, A. Madej, J. Bernard, L. Marmet, and A. Shiner, A narrow linewidth and frequency-stable probe laser source for the $^{88}Sr^+$ single ion optical frequency standard, Appl. Phys. B **95**, 43 (2009).
[56] W. Zhang, W. R. Milner, J. Ye, and S. B. Papp, Cryogenic photonic resonator with $10^{-17}/s$ drift, arXiv:2410.09960.
[57] I. Ito, A. Silva, T. Nakamura, and Y. Kobayashi, Stable cw laser based on low thermal expansion ceramic cavity with 4.9 mHz/s frequency drift, Opt. Express **25**, 26020 (2017).
[58] T. E. Parker, S. R. Jefferts, and T. P. Heavner, Medium-term frequency stability of hydrogen masers as measured by a cesium fountain, in *2010 IEEE International Frequency Control Symposium* (IEEE, Newport Beach, CA, 2010), pp. 318–323.
[59] T. E. Parker, Hydrogen maser ensemble performance and characterization of frequency standards, in *Proceedings of the 1999 Joint Meeting of the European Frequency and Time Forum and the IEEE International Frequency Control Symposium (Cat. No. 99CH36313)* (IEEE, Besancon, France, 1999), Vol. 1, pp. 173–176.
[60] S. J. Griffin, D. Meyer, A. Lemmon, and H. B. Owings, Drift correction for active hydrogen masers, in *2021 Joint Conference of the European Frequency and Time Forum and IEEE International Frequency Control Symposium (EFTF/IFCS)* (IEEE, Gainesville, FL, 2021), pp. 1–6.
[61] W. R. Milner, J. M. Robinson, C. J. Kennedy, T. Bothwell, D. Kedar, D. G. Matei, T. Legero, U. Sterr, F. Riehle, H. Leopardi *et al.*, Demonstration of a timescale based on a stable optical carrier, Phys. Rev. Lett. **123**, 173201 (2019).
[62] W. F. McGrew, X. Zhang, H. Leopardi, R. Fasano, D. Nicolodi, K. Beloy, J. Yao, J. A. Sherman, S. A. Schaeffer, J. Savory *et al.*, Towards the optical second: Verifying optical clocks at the SI limit, Optica **6**, 448 (2019).
[63] C. Grebing, A. Al-Masoudi, S. Dörscher, S. Häfner, V. Gerginov, S. Weyers, B. Lipphardt, F. Riehle, U. Sterr, and C. Lisdat, Realization of a timescale with an accurate optical lattice clock, Optica **3**, 563 (2016).
[64] J. Yao, J. A. Sherman, T. Fortier, H. Leopardi, T. Parker, W. McGrew, X. Zhang, D. Nicolodi, R. Fasano, S. Schäffer, K. Beloy, J. Savory, S. Romisch, C. Oates, S. Diddams, A. Ludlow, and J. Levine, Optical-clock-based time scale, Phys. Rev. Appl. **12**, 044069 (2019).
[65] J. W. Berthold III, S. F. Jacobs, and M. Norton, Dimensional stability of fused silica, invar, and several ultralow thermal expansion materials, Appl. Opt. **15**, 1898 (1976).
[66] M. K. Kreider, C. Fredrick, S. A. Diddams, R. C. Terrien, S. Mahadevan, J. P. Ninan, S. Halverson, C. F. Bender, F. Hearty, D. Mitchell *et al.*, Quantification of broadband chromatic drifts in Fabry–Pérot resonators for exoplanet science, Nat. Astron. **9**, 589 (2025).
[67] D. Lee *et al.* (2026), 10.5281/zenodo.18134864.
[68] S. R. Stein, Frequency and time—their measurement and characterization, in *Precision Frequency Control*, edited by E. A. Gerber and A. Ballato (Academic Press, New York, 1985), Chap. 12.

End Matter

Thermal noise calculation—For cryogenic silicon cavities, the spacer and substrates contribute a negligible amount of noise to the total thermal noise, leaving the coating Brownian noise as the only dominant term. We

TABLE II. Symbols used in Eq. (A1).

Symbol	Description	Value
$S_y(f)$	Fractional frequency noise Power spectral density (Hz^{-1})	
f	Fourier frequency (Hz)	
k_B	Boltzmann constant	1.38×10^{-23} JK^{-1}
T	Temperature	17 K
d_{coat}	Coating thickness	12.0 μm
w	Beam radius at the mirror	293 μm
L	Cavity length	6.02 cm
Y_{coat}	Young's modulus of coating [a]	100 GPa (crystalline) 91 GPa (dielectric)
Y_{sub}	Young's modulus of substrate [b]	188 GPa
σ_{coat}	Poisson's ratio of coating [c]	0.32 (crystalline) 0.2 (dielectric)
σ_{sub}	Poisson's ratio of substrate	0.26
ϕ_{coat}	Mechanical loss factor of coating	see Table III

[a][45] for dielectric, [14] for crystalline.
[b]Along the ⟨111⟩ direction of silicon.
[c][45] for dielectric, [14] for crystalline.

use the formula from Ref. [6], also used in Refs. [14,45], to calculate the coating Brownian noise:

$$S_y(f) = \frac{4k_B T d_{coat}\phi_{coat}}{\pi^2 w^2 Y_{sub} L^2 f}\left[\frac{Y_{coat}}{Y_{sub}}\frac{(1+\sigma_{sub})^2(1-2\sigma_{sub})^2}{1-\sigma_{coat}^2} + \frac{Y_{sub}}{Y_{coat}}\frac{(1+\sigma_{coat})^2(1-2\sigma_{coat})}{1-\sigma_{coat}^2}\right], \quad \text{(A1)}$$

where the meaning of each symbol and its value are summarized in Table II. The mechanical loss factors for dielectric and crystalline coatings are listed in Table III. The $1/f$ dependence of $S_y(f) = h_{-1}f^{-1}$ leads to a constant modified Allan deviation of mod $\sigma_y \approx \sqrt{0.936 h_{-1}}$ [68], shown in Fig. 1 as the thermal noise limit.

Phase noise power spectral density—Figure 4 shows the phase noise power spectral density of the beat note between two lasers stabilized to the 6-cm cavity (Si6) and the 21-cm cavity (Si3). Below 1 Hz Fourier frequency, both cavities contribute similar amounts of noise to the measured noise. Above 1 Hz, the noise of the 6-cm cavity dominates. The phase noise between 10 Hz and 2 kHz is from vibrations and the noise above 2 kHz is from Pound-Drever-Hall lock in-loop noise.

TABLE III. Mechanical loss factors of dielectric SiO_2/Ta_2O_5 and crystalline $GaAs/Al_{0.92}Ga_{0.08}As$ coatings.

Temperature	Dielectric	Crystalline
300 K	4×10^{-4} [29]	2.5×10^{-5} [28]
124 K	2.4×10^{-4} [45]	2.5×10^{-5} [22]
< 17 K	3.2×10^{-4} [45]	5×10^{-5} [42]
		6×10^{-6} [43]
		4×10^{-5} [44]
		$< 2.3 \times 10^{-5}$ [this Letter]

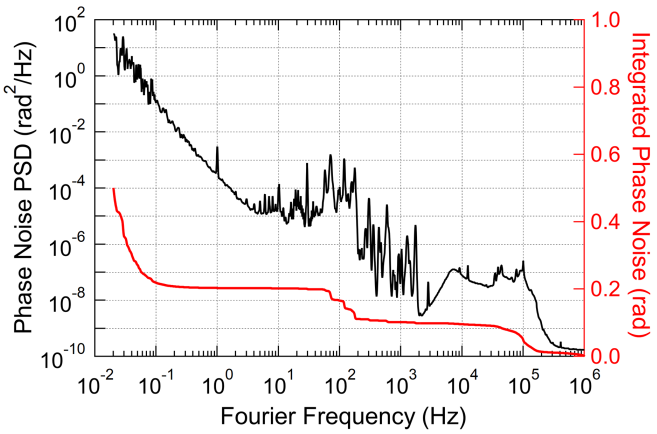

FIG. 4. (black trace, left axis) Phase noise of the beat note between two 1542 nm lasers stabilized to the 6-cm cavity (Si6) and the 21-cm cavity (Si3). (red trace, right axis) Integrated phase noise.